DIGITAL PROTECTION OF POWER TRANSMISSION LINES IN THE PRESENCE OF SERIES CONNECTED FACTS DEVICES

P. K. Dash, A. K. Pradhan, G. Panda
Regional Engineering College, Rourkela
INDIA

A. C. Liew
National University of Singapore
SINGAPORE

ABSTRACT: The presence of series connected FACTS (flexible ac transmission system) devices like TCSC (thyristor controlled series capacitor), TCPST (thyristor controlled phase shifting transformer) and UPFC (unified power flow controller) etc. can drastically effect the performance of a distance relay in a two-terminal system connected by a double-circuit transmission line. The control characteristics of the series connected FACTS devices, their locations on the transmission line, the fault resistance especially the higher ones make this problem more severe and complicated. The fault location with respect to the position of the FACTS devices also greatly influences the trip boundaries of the distance relay. The paper presents apparent impedance calculations for relaying of double-circuit transmission system with varying parameters of the FACTS devices and location. The study reveals the adaptive nature of the protection scheme that necessitaes the use of an ANN based procedure for the generation of trip boundaries during fault conditions.

Key Words- Digital protection, Distance relay, Adaptive setting, FACTS.

I. INTRODUCTION

The possibility of controlling electric power flow in a transmission system by using controllable solid state devices like TCSC and TCPST is well known [1]. These series connected FACTS devices inject a series voltage with the line and thereby modulate the line reactance or the phase shift between the two end voltages. Recent advances in solid-state power electronics technology have made it possible to implement the above devices using power switching voltage source converters. Another versatile FACTS device like UPFC has provided the necessary functional flexibility for optimal power flow control. In the UPFC both active and reactive power flow in the line are controlled through a series and a shunt reactive compensation [1- 2].

The presence of a FACTS device in the fault loop affects both the steady state and transient components in the voltage and current signals at the relaying point. Therefore, the apparent impedance calculations should take into account the variable series voltage source and its angle and shunt current and admittance, if present in the device [3]. However, if the FACTS device is not present in the fault loop, the apparent impedance calculations are similar to the ordinary transmission lines. Thus a decision concerning the relative position of such a device must be considered before the calculation of apparent impedance. Besides the fault resistance magnitude of the arc and system operating condition the apparent impedance seen by a distance relay is influenced greatly by the location and parameters of FACTS device in case of a ground fault. If the impedance seen by a relay is lower or higher than the actual line impedance, the distance relay either overreaches or underreaches. Therefore an adaptive relay setting of the distance protection is required to cope up with the problems of overreach or underreach.

Adaptive reach settings of the distance relays for faults involving high arc resistance have been researched for sometime now [4-9]. Methods for on-line corrections of the trip boundaries are presented in references [5-7]. This paper presents the apparent impedance calculation procedure along with detailed simulation results for distance relaying schemes in which one of the circuits in a double circuit transmission line has a series connected FACTS device. The variations of the device parameters and the locations are found to influence the apparent impedance measurements and trip boundaries to a great extent.

II. APPARENT IMPEDANCE CALCULATION IN THE PRESENCE OF FACTS ELEMENTS

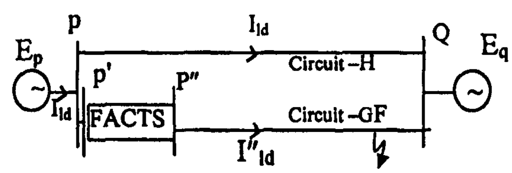

Fig.1. FACTS device at the relaying point in the power system

A double circuit transmission line connecting two sources possessing a TCPST or TCSC or UPFC in one of its circuits at relaying point or midpoint (Fig. 1) is exposed to a single-line-to-ground fault. The apparent impedance as seen by the phase-to-ground relay in such an event taking into account infeed and fault resistance is derived in the following sections.

A. *The TCPST on circuit-G*

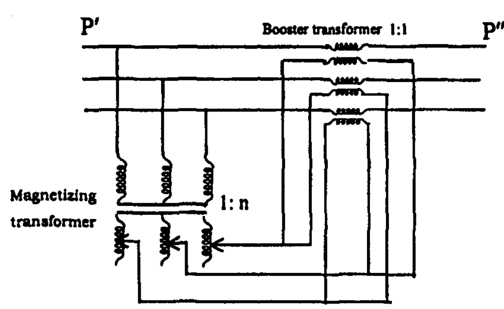

(a)

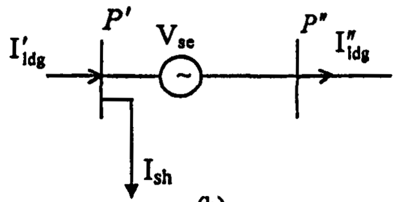

(b)

Fig.2 (a) Basic circuit arrangement of TCPST (b) TCPST model

The TCPST consists of two transformers; a magnetizing transformer connected in parallel and a booster transformer in series to the line (Fig. 2). The current through the magnetizing transformer induces a voltage on the primary side of the booster transformer which is in quadrature with the phase voltages. The basic equations of TCPST for phase-a are:

$$V_{ase} = \gamma e^{j\theta} V_{ap'} \quad (1)$$

Hence $V_{ap'} = C_p V_{ap''}$

$$\text{where } C_p = 1/(1+\gamma e^{j\theta}) \quad (2)$$

$\gamma = \sqrt{3}n$, n = turns ratio of magnetizing transformer

$n = \frac{\tan\phi}{\sqrt{3}}$, the range of ϕ is $-10^0 < \phi < 10^0$ and $\theta = \pm\frac{\pi}{2}$

Equating the complex power between shunt and series branches

$$I_{ash} = -I'_{aldg} e^{j(\phi+\frac{\pi}{2})} \sin\phi \quad (3)$$

Hence

$$I''_{aldg} = I'_{aldg} - I_{ash} = \frac{e^{j\phi}}{t} I'_{aldg} \quad (4)$$

Where $t = \sqrt{1+3n^2}$

1) TCPST at the relaying point :

Considering phase-a to ground fault (Fig. 1) and assigning current between P and P′ as I'_{ldg}, the current relations are

$$I_{ald} = I'_{aldg} + I_{aldh} \quad (5)$$

$$I'_{aldg} = I''_{aldg} + I_{ash} \quad (6)$$

$$I''_{aldg} - I_{aldh} = \frac{\gamma e^{j\frac{\pi}{2}} V_{ap'}}{Z_1} \quad (7)$$

From the above equations we can rewrite

$$I'_{aldg} = C_{cld} V_{ap} \text{ and } I''_{aldg} = C_{cldd} V_{ap} \quad (8)$$

$$\text{where } C_{cld} = \left\{ \frac{\gamma e^{j\frac{\pi}{2}}}{Z_1} + \frac{\frac{1}{h\, e^{-j\delta}} - 1}{Z_{1sp}} \right\} / (1 + \frac{e^{j\phi}}{t})$$

and $C_{cldd} = C_{cld} \frac{e^{j\phi}}{t}$

Again from Fig.1

$$I''_{aldg} = \frac{V_{ap'}/C_p - V_{afd}}{Z_{1pf}} \quad (9)$$

From the above equations we obtain

$$V_{ap} = C_{vp} I_{of} \quad (10)$$

Where $C_{vp} = \frac{-(3R_f + Z_\Sigma)}{(Z_{1pf} C_{cldd} - 1/C_p)}$

$Z_\Sigma = Z'_0 + Z'_1 + Z'_2$ (refer equations 11 and 12) and I_{of} being zero sequence component of fault current. The magnitudes of Z'_0, $Z'_1(Z'_2 = Z'_1)$ are obtained from the equivalent sequence diagrams..

$$Z'_1 = \frac{n(1-n)Z_1}{2} + \frac{(Z_{1sp} + \frac{nZ_1}{2})(Z_{1sq} + \frac{(1-n)Z_1}{2})}{Z_{1sp} + Z_{1sq} + \frac{Z_1}{2}} \quad (11)$$

$$Z'_0 = \frac{\left(Z_{osp} + n\frac{(Z_{0m}+Z_0)}{2}\right)\left(Z_{osq} + \frac{(1-n)(Z_{om}+Z_0)}{2}\right)}{Z_{osp} + Z_{osq} + \frac{Z_{om}+Z_0}{2}} + n(1-n)\frac{(Z_0 - Z_{om})}{2} \quad (12)$$

Where Z_{1sp}, Z_{1sq}, Z_{osp}, Z_{osq} = positive and zero sequence impedances of the sources at the terminals P and Q, respectively. Z_{om} = Zero sequence mutual impedance between circuit G and circuit H. n= per unit distance of the fault point F from the relaying point R.

Also the currents can be expressed as

$$I''_{aldg} = C_{ldd} I_{of} \quad (13)$$

$$I'_{aldg} = C_{ld} I_{of} \quad (14)$$

$$I_{ash} = C_{lsh} I_{of} \quad (15)$$

Where $C_{ldd} = C_{cldd} C_{vp}$, $C_{ld} = C_{cld} C_{vp}$ and $C_{lsh} = C_{ld} - C_{ldd}$

At the relaying point the voltage and current equations of phase-a are:

$$V_{aR} = C_p(3R_f I_{of} + I_{1p''gf} Z_{1pf} + I_{2p''gf} Z_{2p''f} + I_{op''gf} Z_{opf} + I_{oh} Z_{omf} + I''_{aldg} Z_{1pf}) \quad (16)$$

$$I_{aR} = I''_{aldg} + I_{ash} + I_{ap''g} + K_0 I_{0p''gf} \quad (17)$$

Substituting Z_{1pf} by n Z_1, the apparent impedance seen by a-phase to ground relay is

$$Z_a = C_p n Z_1 + \frac{C_p \{3R_f + C_m Z_{0mf} - nZ_1 C_{lsh}\}}{C_{ldd} + C_{lsh} + 2C_1 + C_0(1+K_0)} \quad (18)$$

where $C_m = \frac{nZ_{osq} - (1-n)Z_{osp}}{2Z_{osp} + Z_0 + Z_{om} + 2Z_{osq}}$

$$C_0 = \frac{(2-n)Z_{osq} + (1-n)(Z_0 + Z_{om} + Z_{osp})}{2Z_{osp} + Z_0 + Z_{om} + 2Z_{osq}}$$

and $$C_1 = \frac{(2-n)Z_{1sq} + (1-n)(Z_1 + Z_{1sp})}{2Z_{1sp} + Z_1 + 2Z_{1sq}}$$

From equation 18 it can be observed that if the TCPST is placed at the relaying point on one of the circuits of the double-circuit transmission line, the apparent impedance seen by the relay for a single-line-to-ground fault is influenced by the factor C_p of the TCPST. Also the impedance is influenced by the resistance R_f in the fault path, zero sequence mutual impedance, TCPST shunt branch current, fault location and prefault system condition.

2) TCPST at midpoint of circuit G:

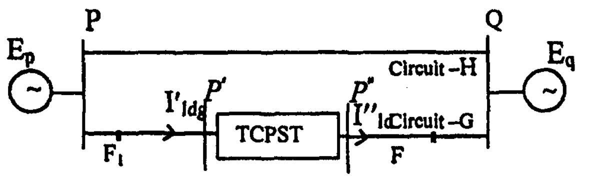

Fig. 3. The power system with TCPST at midpoint of circuit-G

For fault beyond the TCPST (at F_2) the seen impedance (phase-a-to-ground relay) is

$$Z_a = C_p(n - \tfrac{1}{2})Z_1 + \frac{Z_1}{2} + \Delta Z'$$

$$\Delta Z' = \frac{[3R_f C_p + C_m\left(C_p(n-\tfrac{1}{2})Z_{om} + \frac{Z_{om}}{2}\right) - C_{lsh}C_p(n-\tfrac{1}{2})Z_1]}{C_{ldd} + C_{lsh} + 2C_1 + C_0(1+K_{0)})} \quad (19)$$

For fault within the TCPST (at F_1) the apparent impedance equation becomes

$$Z_a = nZ_1 + \frac{\{3R_f + C_m Z_{0mf} - nZ_1(C_{ld} - C_{ldd})\}}{C_{ld} + 2C_1 + C_0(1+K_0)} \quad (20)$$

B. *The TCSC*

The TCSC as shown in Fig. 4 consists of a fixed capacitor and a thyristor controlled reactor that circulates current pulses which add in phase with the line current. This boosts the capacitor voltage beyond the level that would be obtained by the line current alone. The TCSC can be modeled as a variable reactance (both capacitive and inductive) where the net reactance offered by TCSC, X_{net} depends on the conduction angle of the thyristors [10].

1) TCSC at the relaying point:

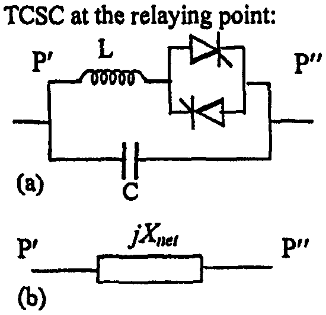

Fig. 4 (a) TCSC circuit arrangement (b) its equivalent representation

The apparent impedance seen by the relay is given by

$$Z_a = nZ_1 + Z_c + \frac{3R_f + C_m nZ_{0m} - C_o(K_0 Z_c)}{C_{ld} + 2C_1 + C_0(1+K_0)} \quad (21)$$

where $Z_c = jX_{net}$ TCSC reactance

2) TCSC at the mid point of circuit G:

Apparent impedance for fault beyond the TCSC (refer Fig. 3)

$$Z_a = (n - \tfrac{1}{2})Z_1 + \frac{Z_1}{2} + Z_c + \Delta Z$$

$$\text{Where } \Delta Z = \frac{[3R_f + C_m\left((n-\tfrac{1}{2})Z_{om} + \frac{Z_{om}}{2}\right) - C_o K_o Z_c]}{C_{ld} + 2C_1 + C_0(1+K_0)} \quad (22)$$

For fault within TCSC; at F_1

$$Z_a = nZ_1 + \frac{3R_f + C_m nZ_{0m}}{C_{ld} + 2C_1 + C_0(1+K_0)} \quad (23)$$

C. The UPFC

The UPFC modeled by two voltage sources is shown in Fig.5. It consists of two converters, one connected in series with the transmission line with a series transformer and the other connected in parallel with the line through a shunt transformer. The series and shunt converters are connected together through a DC capacitor, which also acts as an energy storage device. The series converter introduces a voltage source of variable magnitude and phase angle, while the shunt converter provides the real power balance between the series converter and the power system.

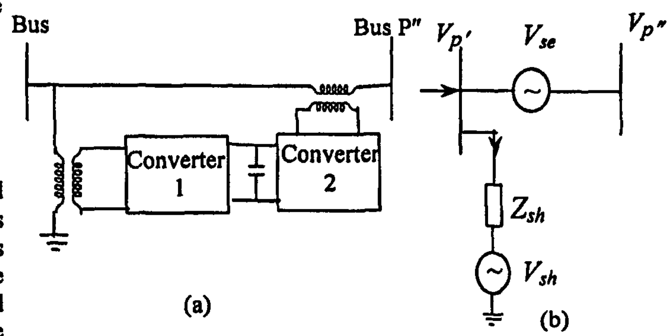

Fig. 5. (a)Basic circuit arrangement of UPFC
(b) its equivalent voltage representation

For apparent impedance calculations, the UPFC model equations for the a-phase are

$$V_{ap'} = C_p V_{ap''} \quad (24)$$

where $C_p = 1/(1+\gamma e^{j\theta})$, $\gamma = \frac{|V_{ase}|}{|V_{ap'}|}$

The magnitude of V_{ase} can be controlled by varying the dc voltage and firing angle of the series voltage source converter and θ varies from 0 to 2π radians. The shunt current is obtained as

$$I_{ash} = \left(V_{ap'} - V_{ash}\right)/Z_{sh}$$
$$V_{ash} = V_{ap'}/C_{sh} \qquad (25)$$

Where V_{ash} =shunt converter voltage, C_{sh}=voltage ratio$(V_{ap'}/V_{ash})$ and Z_{sh} is its impedance. Assume E_{ap} as the equivalent voltage source of the a-phase at the terminal P. Let the relation between bus voltage at P and E_{ap} be

$$V_{ap} = h\, e^{-j\delta} E_{ap} \qquad (26)$$

Where h is the amplitude ratio (V_{ap}/E_{ap}) and δ is the angle between the source voltage and bus voltage at P. The magnitude of shunt converter voltage source V_{sh} is computed from the power balance equation;

$$\mathrm{Re}(V_{ap'} I_{ash}^{*}) = \mathrm{Re}(\gamma V_{ap'}\, e^{j\theta} I''^{*}_{aldg}) \qquad (27)$$

For the two locations of the UPFC on circuit-G the equations are similar to the cases of TCPST.

III. SIMULATION RESULTS

The data of the transmission system used for the simulation purpose is given below:

System voltage =400kV, Length of the line=200km

Positive sequence impedance of each line =$0.2875\angle 86^0$ Ω/km

Zero sequence impedance of each line =$0.8735\angle 83^0$ Ω/km

Zero sequence mutual impedance of line=$0.71\angle 76^0$ Ω/km

Parameters for sources at P and Q are:

$Z_{1sp}=19.5\angle 85^0\,\Omega$, $Z_{1sq}=9.75\angle 85^0\,\Omega$

$Z_{0sp}=5.54\angle 62^0\,\Omega$, $Z_{0sq}=2.77\angle 62^0\,\Omega$

Amplitude ratio between source voltages at P and Q= 0.95

Load angle between sources = 20^0

A single line to ground fault in phase-a is assumed to occur at a distance of 95% of the length from the relaying point in circuit-G where the FACTS element is placed. For both the positions of the FACTS element computations were carried out to evaluate apparent impedance with different fault path resistance values (0 -200Ω). System conditions remaining the same some of the results showing apparent reactance and resistance (the real and imaginary parts of Z_a respectively) are tabulated at R_f=18Ω.

A. *In presence of TCPST*

Table 1 TCPST at relaying point, R_f=18Ω

ϕ	θ =90⁰		θ =-90⁰	
	X_aΩ	R_aΩ	X_aΩ	R_aΩ
10⁰	27.76	81.73	68.50	96.38
5⁰	34.13	88.33	54.48	96.09
0⁰	42.47	94.38	42.47	94.38
-5⁰	31.95	91.70	53.30	99.12
-10⁰	22.58	88.21	66.96	101.22

Table 2 TCPST at midpoint, R_f=18Ω

ϕ	θ =90⁰		θ =-90⁰	
	X_aΩ	R_aΩ	X_aΩ	R_aΩ
10⁰	29.42	79.15	66.54	104.57
5⁰	34.82	86.81	52.68	100.34
0⁰	42.47	94.38	42.47	94.38
-5⁰	33.71	88.38	54.12	100.55
-10⁰	26.86	82.09	68.70	104.67

At relaying point for θ =90⁰ (Table 1) the reactance and the resistance values decrease for higher value of ϕ (both positive and negative values). For example the reactance value reaches to 27.76Ω from 42.47Ω and the resistance to 81.73Ω from 94.38Ω at ϕ=10⁰ and at ϕ=-10⁰ the reactance to 22.58Ω and resistance to 88.21Ω. The reverse is the trend for θ =90⁰; the reactance value goes up to 68.50Ω and resistance to 96.38Ω for the same ϕ=10⁰ and incase of ϕ=-10⁰ reactance is 66.96Ω and resistance 101.22Ω. For the TCPST at mid point (Table 2) with same R_f =18Ω and θ =90⁰ the reactance decreases to 29.42Ω from 42.47Ω and the resistance to 79.15Ω from 94.38Ω. But for θ =-90⁰ a reverse trend is observed and the reactance increase to 66.54Ω and also the resistance to 104.57Ω.

B. *In presence of TCSC*

Table 3 TCSC with R_f=18Ω

compe-nsation %	relay point		mid point	
	X_aΩ	R_aΩ	X_aΩ	R_aΩ
30	33.59	75.44	33.59	75.44
15	38.10	84.95	38.10	84.95
0	42.47	94.38	42.47	94.38
-15	46.66	103.18	46.66	103.68
-30	50.67	112.83	50.67	112.83

Unlike the TCPST the position of TCSC does not have any influence in seen impedance at 95% of the line length. As expected with capacitive mode of operation the reactance should decrease, for 30% compensation (capacitive) the reactance decreases to 33.59Ω from 42.47Ω and resistance to 75.44Ω from 94.38Ω. In case of –30% compensation level the reactance increases to 50.67Ω and so also the resistance to 112.83Ω.

C. *In presence of UPFC*

The value of γ of the UPFC is varied between 0 and 0.5, while that of θ is varied between 0⁰ and 360⁰. The shunt voltage source converter has an impedance of $Z_{sh}=5\angle 85.5^\circ\Omega$. Table 4 shows the apparent resistance R_a and reactance X_a seen by the relay for values of γ varying from 0 to 0.5 and θ at discrete angles of 0⁰, 90⁰ and 270⁰. The fault resistance R_f is assumed to be 18Ω. The location of the UPFC is now changed to the midpoint of the transmission line of the circuit G. Table 2 exhibits the variations in R_a and X_a for different values of γ and θ.

Table 4 UPFC at relaying point, R_f=18Ω

γ	θ =0⁰		θ =90⁰		θ =270⁰	
	X_aΩ	R_aΩ	X_aΩ	R_aΩ	X_aΩ	R_aΩ
0.0	42.47	94.38	42.47	94.38	42.47	94.38
0.1	41.45	46.89	35.44	80.50	56.12	87.27
0.2	33.32	30.37	26.18	80.15	71.13	92.05
0.3	27.74	22.72	19.61	76.13	87.28	87.27
0.4	23.95	18.39	14.57	71.79	102.86	77.05
0.5	21.25	15.62	10.66	67.59	115.51	61.98

Table 5 UPFC at midpoint, R_f=18Ω

γ	θ=0°		θ=90°		θ=270°	
	X_aΩ	R_aΩ	X_aΩ	R_aΩ	X_aΩ	R_aΩ
0.0	42.47	94.38	42.47	94.38	42.47	94.38
0.1	49.90	63.73	35.71	82.63	55.57	99.08
0.2	48.81	48.19	28.43	77.44	71.62	101.75
0.3	46.88	39.29	23.94	71.10	89.99	99.51
0.4	45.19	33.58	20.98	65.26	108.17	90.82
0.5	43.82	29.59	19.09	60.09	122.79	76.08

With the UPFC at the relaying point (Table 4) and θ =0° the resistance seen by the phase-a ground relay decreases considerably whereas the reactance increases up to γ=0.1 and then decreases significantly. For θ =90° the reactance decreases from 42.47Ω to 10.66Ω and also the resistance falls to 67.59Ω from 94.38Ω. However at θ =270° the reactance increases drastically, but the resistance shows a complex variation. Table 5 for mid point location of the UPFC depicts that at θ =0° the resistance value decreases considerably but the reactance varies in a complex manner. At θ =90° the reactance reaches to 19.02Ω from 42.47Ω and the resistance also decreases to 60.09Ω from 94.38Ω. In case of θ =270° the X_a increases drastically but R_a shows a complex variation. These observations clearly demonstrate that the presence of UPFC introduces a capacitive or inductive reactance to the line depending on its parameters γ and θ and location.

IV. TRIP CHARACTERISTICS

Keeping the system operating condition same trip boundaries are generated considering line-to-ground fault for one of the circuit by varying fault distance in km from 0 to 95% of the line and fault path arc resistance from 0 to 200Ω. Fig. 6 depicts the trip characteristic without the presence of any FACTS element for line-to-ground fault. However, if any of the FACTS elements is located at the midpoint the trip characteristic exhibits two different trip boundaries. The upper one is for faults between the midpoint and to 95% of the line length and the lower characteristic is due to the fault location lying between the relaying point to the midpoint.

A. *In presence of TCPST*

Figs. 7 and 8 represent the trip boundary with the presence o TCPST for the same system condition as in UPFC study for different values of and θ (90° and -90°) at ϕ =10° . For ϕ=10° and θ =90° (Fig. 7) the trip characteristic for TCPST at relaying point shifts downward and for mid point case the trip area decreases. At both the locations, the R_a value is decreased.. For ϕ=10° and θ =-90° (Fig. 8) the trip areas are increased considerably and the X_a value goes as high as 160Ω and R_a reaches 400Ω. The trip boundaries for TCPST demonstrate that they are greatly influenced by the position and parameters of TCPST.

B. *In presence of TCSC*

Trip characteristics in the presence of TCSC on one of the circuit are shown in Figs. 9 for capacitive (30%) mode of operations. In the figure, the upper boundaries for TCPST at mid point and relaying point converge. In Fig. 9 the reactance value is decreased and the lower boundary for relaying point is well below that of the mid point case. Therefore it can be concluded that the location and level of compensation of TCSC influences the trip boundary settings.

C. *In presence of UPFC*

Figs. 10 and 11 represent the trip boundaries for line-to-ground fault with the presence of UPFC either at the relaying point or midpoint of circuit G for θ values of 0°and 90° keeping γ unchanged (γ=0.5). In Fig.10 it is observed that for θ=0° and UPFC at both the locations, the X_a value decreases for smaller R_f and increases for higher R_f. However, for the above cases, the R_a value is decreased significantly. With same system conditions with UPFC at the relaying point the trip area is reduced which is not the case for midpoint location of UPFC. Fig. 11 demonstrates that for θ=90° the upper boundary decreases with higher R_f for both the locations of UPFC. These figures clearly show that the UPFC parameters and position modulate the trip boundary set for line to ground fault protection.

V. DISCUSSIONS

It is evident from the two preceding sections that the presenc of FACTS elements in a transmission system affects the tri boundary set for single-line-to-ground fault considerably. No only the parameters of the element, its location on the line als influences the trip characteristics substantially. In case o UPFC the influencing parameters are γ and θ, that for TCPS are ϕ and θ and for the TCSC it is only the compensatio level. In all the observations only two positions of the FACT elements on the line are envisaged and in all cases th characteristics differ with respect to the location of th element. Therefore in an adaptive protection for a transmissio system possessing such a FACTS device the trip boundar needs to be adapted with the mentioned influencin parameters besides the system operating conditions. Artifici intelligence techniques such as neural network, fuzzy logi system etc. may dictate a solution to the above comple protection problem considering the influencing parameters a ome of the inputs.

VI. CONCLUSIONS

Apparent impedance calculations for a double-circu transmission line operating with series connected FACT devices are presented. The presence of a FACTS device lik UPFC, TCPST or TCSC on a line can substantially influenc the apparent impedance seen by a distance relay. Th phenomenon has been clearly demonstrated in this paper b varying the parameters of the FACTS element, its locatio fault resistance along with source impedance and oth uncertainties for line to ground fault. The ideal trip boundari derived are clearly showing the influence of FACTS devi operating parameters. In real-time applications the boundaries need to be generated adaptively for issuing t necessary trip commands to the circuit breakers.

VII. REFERENCES

[1] M. Noroozian, L.Angquist, M.Ghandhari, and G.Anderson, "Improving Power System Dynamics by series connected FACTS devices", IEEE Trans. on Power Delivery, Vol. 12, No. 4, 1997,pp.1635-1641

[2] K. R. Padiyar and A.M. Kulkarni, "Control, Design and Simulation of Unified Power Flow Controller", IEEE Trans. on Power Delivery, Vol.13, No. 4, 1998, pp.1348-1354.

[3] A.A. Girgis, A.A. Sallam and A.K. El-Din, "An Adaptive Protection Scheme for Advanced Series Compensated (ASC) Transmission Lines, IEEE Trans. on Power Delivery, Vol. 13, No. 1, 1998,pp. 414-420.

[4] A.K. Jampala, S.S. Venkata and M.J. Damborg, "Adaptive transmission protection: Concepts and Computational issues", IEEE Trans. on Power Delivery, Vol.4, No. 1, 1989, pp. 177-185.

[5] Z. Zhizha, and C. Deshu, "An adaptive approach in Digital Distance protection", IEEE Trans. on Power Delivery, Vol. 6, No. 1, 1991, pp.135-142.

[6] Y. Q. Xia, K. K. Li and A.K. David, Adaptive relay setting for stand-alone digital distance protection, IEEE Trans. on Power Delivery, Vol. 9, No. 1, 1993, pp. 480-491.

[7] P.J. Moore, R.K. Aggarwal, H. Jiang and A.T. Johns, "New Approach to Distance Protection for Resistive Double-Phase to Earth Faults using Adaptive Techniques", IEE Proc.-Gener. Transm. Distrib., Vol.141, No.4, 1994, pp.369-376.

[8] D.L. Waikar, S. Elangovan, and A.C. Liew, "Further Enhancements in the Symmetrical Components based Improved fault Impedance Estimation Method Part-I. Mathematical Modeling, Electric Power Systems Research, Vol.40, 1997, pp. 189-194.

[9] G. Jongepier, and L.V.D. Sluis, "Adaptive Distance Protection of a Double Circuit Line", IEEE Trans. on Power Delivery, Vol. 9, No. 3, 1994, pp.1289-1297

[10] E. V. Larsen, K.Clark, S. A. Miske, and J.Urbanek, "Characteristics and Rating Consideration of Thyristor Controlled Series Compensation", IEEE Trans. on Power Delivery, 1994, 9, (2), pp.992-999

VIII. BIOGRAPHIES

P. K. Dash is a Professor of Electrical Engineering and Chairman of the Centre of Applied Artificial Intelligence, Regional Engineering College, Rourkela, India.

A. K. Pradhan is a lecturer in the department of Electrical Engineering, University College of Engineering, Burla, India.

G. Panda is Professor and Head of the department of Applied Electronics and Instrumentation Engineering, Regional Engineering College, Rourkela, India.

A. C. Liew is with department of Electrical Engineering, National Institute of Singapore, Singapore.

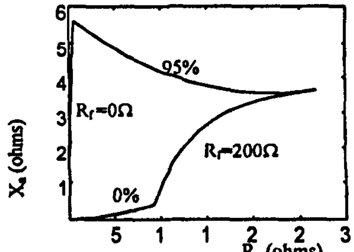

Fig. 6. Trip characteristic without FACTS device for LG fault

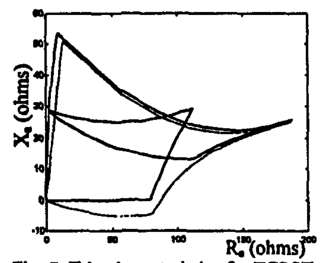

Fig. 7. Trip characteristics for TCPST $\phi=10^0$, $\theta=90^0$ at relay point —— at mid point——

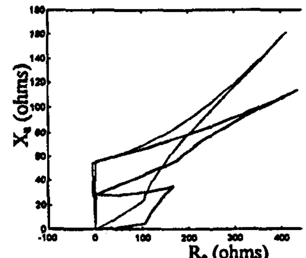

Fig.8. Trip characteristics for T $\phi=10^0$, $\theta=90^0$ at relay point ——at mid point

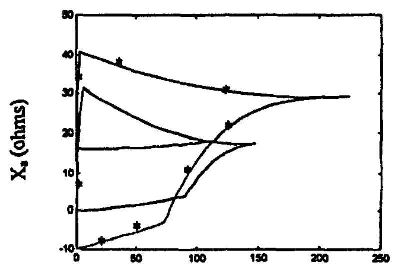

R_a (ohms)
Fig. 9. Trip characteristics for TCSC with 30% compensation at relay point *— at mid point ——

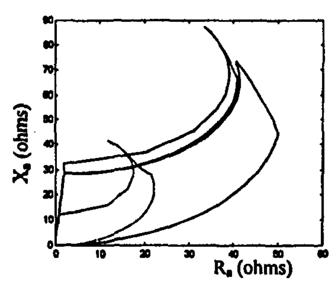

Fig. 10. Trip characteristics for UPFC $\Upsilon=0.5$, $\theta=0^0$ at relay point —— at mid point ——

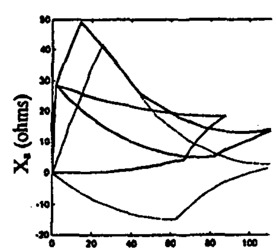

R_a (ohms)
Fig. 11. Trip characteristics i $\Upsilon=0.5$, $\theta=90^0$ at relay point — at mid poi